

# Transverse Fresnel-Fizeau drag effects in strongly dispersive media.

I. Carusotto,<sup>1,\*</sup> M. Artoni,<sup>2,3</sup> G. C. La Rocca,<sup>4</sup> and F. Bassani<sup>4</sup>

<sup>1</sup>*Laboratoire Kastler Brossel, École Normale Supérieure,  
24 rue Lhomond, 75231 Paris Cedex 05, France*

<sup>2</sup>*INFM, Department of Chemistry and Physics of Materials, Via Valotti 9, 25133 Brescia, Italy*

<sup>3</sup>*INFM, European Laboratory for non-Linear Spectroscopy,  
Via N. Carrara 1, 50019 Sesto Fiorentino, Italy.*

<sup>4</sup>*Scuola Normale Superiore and INFM, Piazza dei Cavalieri 7, I-56126 Pisa, Italy*

(Dated: October 29, 2018)

A light beam normally incident upon an uniformly moving dielectric medium is in general subject to bendings due to a transverse Fresnel-Fizeau light drag effect. In conventional dielectrics, the magnitude of this bending effect is very small and hard to detect. Yet, it can be dramatically enhanced in strongly dispersive media where slow group velocities in the m/s range have been recently observed taking advantage of the electromagnetically induced transparency (EIT) effect. In addition to the usual downstream drag that takes place for positive group velocities, we predict a significant anomalous upstream drag to occur for small and negative group velocities. Furthermore, for sufficiently fast speeds of the medium, higher order dispersion terms are found to play an important role and to be responsible for peculiar effects such as light propagation along curved paths and the restoration of the spatial coherence of an incident noisy beam. The physics underlying this new class of slow-light effects is thoroughly discussed.

PACS numbers: 42.50.Gy , 42.25.Bs

## I. INTRODUCTION

A constant effort has always be devoted to the search for new effects and materials to control the propagation of light waves. Over the past few years, in particular, the use of quantum interference has led to an astonishing control of light waves propagating through specific classes of atomic and solid state media. These materials exhibit superior properties that cannot be found in conventional ones. *Slow light* propagation at group velocities as small as 1 m/s, e.g., has been observed in experiments with Bose-Einstein condensates of sodium atoms [1, 2], in hot rubidium vapors [3, 4] as well as in solid doped Pr:Y<sub>2</sub>SiO<sub>5</sub> [5] crystals and Ruby [6]. Reversible *stopping* of a laser pulse [7] in ultracold and hot alkali vapors [8, 9] as well as in Pr:Y<sub>2</sub>SiO<sub>5</sub> crystal has also been observed [5].

Light stopping and slow-light propagation effects originate from electromagnetically induced transparency (EIT). Such a widely discussed phenomenon arises from quantum interference and is characterized by a strong enhancement of the refractive index dispersion within a narrow frequency window around the medium resonance where absorption turns out to be largely quenched. The study of such a phenomenon goes back to the late seventies when non-absorbing resonances in atomic sodium have first been observed by Gozzini's group and later interpreted in terms of coherent population trapping [10, 11, 12].

The interest for such a phenomenon has revived [13] over the past decade and has now become a rather top-

ical area of research [14, 15], much work being done on fundamental issues: high nonlinear coupling between weak fields and quantum entanglement of slow photons [16, 17, 18], entanglement of atomic ensembles [19], quantum memories [20] and enhanced acousto-optical effects [21], just to mention a few. In particular, a strict analogy between slow-light in moving media and light propagating in curved space-times has been unveiled and some of its consequences have been recently discussed [22, 23, 24, 25, 26, 27, 28].

Recently it has been also anticipated in [29] that EIT media are ideal candidates for the observation of extremely low and negative group velocities and (apparently) superluminal behaviour. In such media, the group velocity can in fact be readily tuned over a wide range of negative values directly by varying the coupling and probe detunings in a standard three-level  $\Lambda$  configuration.

Although most slow light and negative group velocity experiments have dealt with the basic problem of a light pulse delay during its propagation across the dispersive medium, ultraslow positive or negative group velocities can have interesting consequences in many different scenarios. In this paper we present a thorough investigation of slow-light propagation through a moving medium. Specifically, we examine a configuration in which a highly dispersive EIT medium which moves with uniform velocity and normally <sup>1</sup> to an incident light beam of finite spa-

---

<sup>1</sup> A configuration in which the medium is set to move parallel to the probe light-beam, leading to the more familiar *longitudinal* Fresnel-Fizeau effect, has been studied in [30]. Also in this configuration, the magnitude of the light-drag effect is predicted to

---

\*Electronic address: Iacopo.Carusotto@lkb.ens.fr

tial extent. The same geometry was adopted in the early seventies by Jones in his pioneering work on the *transverse* Fresnel-Fizeau light drag effect [31, 32] leading to the observation of a very small downstream bending, i.e., in the direction of motion, of a light ray. The use of a strongly dispersive medium supporting slow light, rather than the non-dispersive glassy material used by Jones, will not only allow for a remarkable enhancement of the drag effects but also for qualitatively new features.

The possibility of having light propagating with small negative group velocities across the dragging medium is predicted to yield large *upstream* light bendings, i.e. in the direction opposite to that of the medium. The phenomenology of such an anomalous Fresnel-Fizeau light drag effect, which has been the subject of an old controversy during the late seventies [33, 34], is here discussed in detail unwinding some of its controversial aspects.

For sufficiently fast dragging speeds, the correct description of the slow light transverse dragging effect requires that absorption dispersion and group velocity dispersion be taken into account. As we shall see below, it turns out that these higher-order dispersion terms introduce new and peculiar features, such as propagation along curved light paths and the restoration of the spatial coherence of a noisy beam. All the numerical results presented in this paper have been obtained using realistic parameters taken from slow-light experiments in ultracold atomic clouds [1]. Since the physics of the system is essentially determined by the electromagnetically induced transparency effect, the physical features here discussed are however extremely general and hold through also for the recently prepared solid state EIT media.

The paper is organized as follows. In sec. II we introduce the physical system and we present the model used for our predictions. The general theory of the transverse Fresnel-Fizeau light drag effect is presented in sec. III. These general results are specialized to the case of a strongly dispersive dressed medium driven into a  $\Lambda$  configuration by a resonant and non-resonant coupling beam respectively in sec. IV and in sec. V: in the former case, the group velocity is small and positive, so the transverse Fresnel drag occurs in the usual downstream direction; in the latter case, the negative group velocity is shown to give an anomalous upstream Fresnel drag. In sec. VI we proceed to discuss some effects which arise from the inclusion of higher order dispersion terms. We carry out a complete analysis for two specific instances. In one case, the beam spectrum reshaping due to absorption and group velocity dispersion, which makes the average group velocity to bend during propagation, is seen to lead to curved light paths. In the other, the frequency dispersion of absorption is seen to act as a filter for spatial fluctuations of the beam, whose space coherence properties improve as it propagates through the medium. Fi-

nally, a summary of the work is given in sec. VII where conclusions are also drawn.

## II. THE MODEL AND GENERAL THEORY

We consider a monochromatic *probe* light beam of frequency  $\omega_0$  propagating along the  $z$  axis and normally incident upon a homogeneous dielectric medium uniformly moving along the  $x$  direction as shown in fig.1. We here denote with  $L$  the thickness of the slab and with  $v$  its velocity  $v \ll c$ . The probe beam has a Gaussian profile centered in  $(x_0, y_0)$  so that at  $z = 0$  one has,

$$E_0(x, y) = E_0 e^{-[(x-x_0)^2 + (y-y_0)^2]/2\sigma_0^2}, \quad (1)$$

where  $\sigma_0$  is the beam waist. The corresponding Fourier transform  $\tilde{E}_0(k_x, k_y)$  of  $E_0(x, y)$  is then a Gaussian of width  $\sigma_0^{-1}$ .

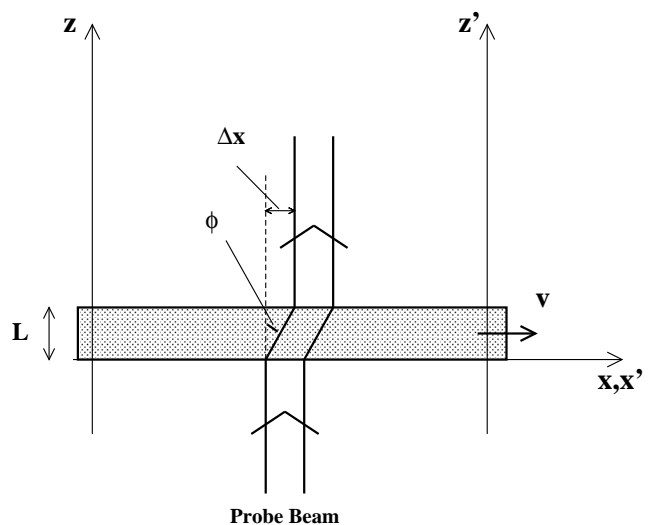


FIG. 1: Scheme of the experimental set-up under consideration.

In the following we shall always restrict our attention to the case of a weak probe beam, which allows us to apply linear response theory and describe the polarization of the medium by means of a dielectric function  $\epsilon$ . Assuming for simplicity a non-magnetic ( $\mu = 1$ ) and isotropic  $\epsilon_{i,j} = \epsilon \delta_{i,j}$  medium, the scalar dielectric function  $\epsilon$  completely characterizes the linear polarization of the medium in its rest frame  $\Sigma'$ . Spatial locality of the dielectric polarization will also be assumed, i.e.  $\epsilon$  will be taken to depend on the frequency  $\omega'$  but not on the wave-vector  $\mathbf{k}'$ . Primed quantities will refer to the medium rest frame  $\Sigma'$ , while the non-primed ones will refer to the laboratory frame  $\Sigma$ . The linearity of the optical response and the translational invariance of the system on the  $(x, y)$  plane allow us to decompose the incident field in its Fourier components in the  $(x, y)$  plane, to propagate each of them independently from the others, and to

be strongly enhanced in the slow light regime.

finally reconstruct the transmitted beam profile by using an inverse Fourier transform.

In the  $\Sigma'$  frame, the dispersion law inside the medium has the usual form:

$$\epsilon(\omega')\omega'^2 = c^2(k_x'^2 + k_y'^2 + k_z'^2). \quad (2)$$

Since the slab speed  $v \ll c$ , the linearized form of the Lorentz transformations can be used, namely:

$$\omega' = \omega - k_x v \quad (3)$$

$$k_x' = k_x - \frac{\omega}{c^2} v \quad (4)$$

$$k_{y,z}' = k_{y,z}. \quad (5)$$

Notice that even though the medium does exhibit spatial dispersion in its rest frame  $\Sigma'$ , spatial dispersion arises however in the laboratory frame  $\Sigma$  from the dependence of  $\omega'$  on  $k_x$ <sup>2</sup>. By inserting the transformations (3-5) into the dispersion law (2), one obtains the following expression:

$$\frac{(\omega - k_x v)^2}{c^2} \epsilon(\omega - k_x v) = \left(k_x - \frac{\omega v}{c^2}\right)^2 + k_y^2 + k_z^2. \quad (6)$$

This equation represents the dispersion law in  $\Sigma$  and can be used to determine the propagation of the light beam across the slab. Knowing the frequency  $\omega_0$  and the transverse components  $k_{x,y}$  of the wavevector allows us to obtain from (6) the  $z$  component  $k_z^{(in)}$  of the wave-vector inside the medium:

$$k_z^{(in)}(k_x, k_y) = \sqrt{\left(\frac{\omega_0 - k_x v}{c}\right)^2 \epsilon(\omega_0 - k_x v) - \left(k_x - \frac{\omega_0 v}{c^2}\right)^2 - k_y^2}, \quad (7)$$

as well as in the external free space:

$$k_z^{(out)}(k_x, k_y) = \sqrt{\frac{\omega_0^2}{c^2} - k_x^2 - k_y^2}. \quad (8)$$

The profile of the transmitted beam can then be obtained by decomposing the field in its Fourier components at transverse wavevector  $(k_x, k_y)$  and propagating each of them independently with the wave-vectors (7) and (8). Since the energy flux must be along the positive  $z$  axis, the roots with positive real part  $\text{Re}[k_z^{(in,out)}] > 0$  have to be taken<sup>3</sup>.

<sup>2</sup> In the rest frame  $\Sigma'$ , the dielectric polarization of a medium with frequency dispersion depends on the retarded values of the electric field at the same spatial position. As seen from the laboratory frame  $\Sigma$ , the polarization at a given point will thus depend on the electric field at different spatial positions, which means that a moving medium shows a spatial dispersion in  $\Sigma$  even if it is only temporally dispersive in the rest frame  $\Sigma'$ .

<sup>3</sup> As the reflection amplitude is proportional to  $\epsilon - 1$ , the approximation of neglecting interface reflections is a reasonable approximation in the case of an ultra cold atomic gas on which the present paper is focussed. On the other hand, a more complete theory including the possibility of multiple interface reflections is required in the case of a solid state medium.

For each component, the amplitude at the position  $0 \leq z \leq L$  inside the slab is given by:

$$\tilde{E}(k_x, k_y; z) = e^{i\Phi(k_x, k_y; z)} \tilde{E}_0(k_x, k_y) \quad (9)$$

with a phase  $\Phi$ :

$$\Phi(k_x, k_y; z) = k_z^{(in)}(k_x, k_y) z \quad (10)$$

Notice that the wavevector  $k_z^{(in)}(k_x, k_y)$  as well as the phase  $\Phi(k_x, k_y; z)$  are generally complex quantities; their imaginary parts vanish only for non-absorbing, non-amplifying medium. Past the slab, the transmitted amplitude at the position  $z > L$  is given by the same equation (9) with the phase  $\Phi$  now given by:

$$\Phi(k_x, k_y; z) = k_z^{(in)}(k_x, k_y) L + k_z^{(out)}(k_x, k_y) (z - L). \quad (11)$$

The spatial profile of the transmitted beam at any point  $z$  can then be obtained taking the inverse Fourier transform of (9),

$$E(x, y, z) = \int \frac{dk_x dk_y}{2\pi} e^{i(k_x x + k_y y)} e^{i\Phi(k_x, k_y; z)} \tilde{E}_0(k_x, k_y). \quad (12)$$

### III. THE TRANSVERSE FRESNEL-FIZEAU DRAG EFFECT

Provided that the incident beam waist  $\sigma_0$  is wide enough, only a very small window of wave-vectors  $(k_x, k_y)$  around  $k_{x,y} = 0$  is effectively relevant to the propagation dynamics and one can safely expand the phase (11) in powers of  $k_{x,y}$  so that to the lowest order one has:

$$\Phi(k_x, k_y; z) = \frac{\omega_0}{c} \sqrt{\epsilon(\omega_0)} \left[ 1 - \frac{k_x v}{\omega_0} \left( 1 - \frac{1}{\epsilon(\omega_0)} \right) - \frac{k_x v}{2\epsilon(\omega_0)} \frac{d\epsilon}{d\omega} \right] L + \frac{\omega_0}{c} (z - L). \quad (13)$$

The position of the center  $(x_c, y_c)$  of the resulting wave packet at a given  $z$  can be obtained inserting the expansion (13) into (12) and then invoke the so-called *stationary-phase* principle. This states that the integral in (12) has its maximum value at those points  $(x_c, y_c)$  for which constructive interference between the different Fourier components occurs, that is at those points at which the phase of the integrand is stationary [35]:

$$\frac{\partial}{\partial k_{x,y}} \left( \text{Re}[\Phi(k_x, k_y; z)] + k_x x_c + k_y y_c \right) \Big|_{k_x=k_y=0} = 0. \quad (14)$$

Inserting into (14) the expression of the phase (13) and assuming the imaginary part  $\epsilon_i$  of  $\epsilon = \epsilon_r + i\epsilon_i$  to be negligible, one finds that in the laboratory frame  $\Sigma$  the beam

propagates inside the moving slab at a non-vanishing angle  $\theta$  with respect to the normal  $z$  direction given by:

$$\tan \theta = \frac{v}{c} \left[ \sqrt{\epsilon_r(\omega_0)} + \frac{\omega_0}{2\sqrt{\epsilon_r(\omega_0)}} \frac{d\epsilon_r}{d\omega} - \frac{1}{\sqrt{\epsilon_r(\omega_0)}} \right] = \frac{v}{c} \left[ \frac{c}{v'_{\text{gr}}} - \frac{v'_{\text{ph}}}{c} \right]. \quad (15)$$

Here  $v'_{\text{gr}}$  and  $v'_{\text{ph}}$  denote respectively the group and phase velocities in the medium rest frame  $\Sigma'$ :

$$v'_{\text{ph}} = \frac{c}{\sqrt{\epsilon_r(\omega_0)}} \quad (16)$$

$$v'_{\text{gr}} = \frac{c}{\sqrt{\epsilon_r(\omega_0)} + \frac{\omega_0}{2\sqrt{\epsilon_r(\omega_0)}} \frac{d\epsilon_r}{d\omega}}. \quad (17)$$

This deflection of the light beam can be interpreted as a *transverse* Fresnel-Fizeau drag effect, in which the beam of light is dragged by the transverse motion of the medium. After exiting from the rear surface of the slab, the beam again propagates along the normal direction. Its center, however, turns out to be laterally shifted by an amount,

$$\Delta x = Lv \left[ \frac{1}{v'_{\text{gr}}} - \frac{v'_{\text{ph}}}{c^2} \right]. \quad (18)$$

along a direction parallel to the medium velocity. This expression is in agreement with the ones derived by Player and by Rogers [36, 37].

While the group velocity direction inside the moving medium makes a finite angle  $\theta$  with respect to the normal, the transverse  $x$  and  $y$  components of the phase velocity are always vanishing in the laboratory frame  $\Sigma$  because the light beam is normally incident on the slab and the transverse wave vector is conserved at the interface. The non-parallelism of the group and phase velocities arises then from the effective spatial dispersion acquired in the laboratory frame  $\Sigma$  by the moving medium<sup>4</sup>. Indeed, one can calculate the group velocity  $\mathbf{v}_{\text{gr}} = \nabla_{\mathbf{k}}\omega(\mathbf{k})$  at  $k_{x,y} = 0$  directly from the dispersion law (6) to obtain for each component:

$$v_{\text{gr},x} = v \left( 1 - \frac{1}{\epsilon + \frac{\omega}{2} \frac{d\epsilon}{d\omega}} \right) = v \left( 1 - \frac{v'_{\text{gr}} v'_{\text{ph}}}{c^2} \right) \quad (19)$$

$$v_{\text{gr},y} = 0 \quad (20)$$

$$v_{\text{gr},z} = \frac{c}{\sqrt{\epsilon} + \frac{\omega}{2\sqrt{\epsilon}} \frac{d\epsilon}{d\omega}} = v'_{\text{gr}}. \quad (21)$$

The non-vanishing value of  $v_{\text{gr},x}$  is responsible for the transverse Fresnel-Fizeau drag. The value of  $\tan \theta =$

$v_{\text{gr},x}/v_{\text{gr},z}$  obtained from (19) and (21) agrees indeed with (15).

Another picture of this drag effect can be obtained by working in the rest frame  $\Sigma'$  [38]. Because of the aberration of light [35], the direction of the incident beam makes an angle  $\theta'_{\text{inc}} = -v/c$  with the normal<sup>5</sup>. In the rest frame  $\Sigma'$ , the group and phase velocities inside the medium are parallel to each other and make an angle  $\theta'_{\text{refr}} = -v/(c\sqrt{\epsilon})$  with the normal according to Snell's law. The modulus of the group velocity in  $\Sigma'$  is given by (17). By Lorentz-transforming back the group velocity to the laboratory frame  $\Sigma$ , it is easy to check that the same deflection angle as in (15) is obtained.

As one can see from the explicit expression (18) the magnitude of the transverse drag  $\Delta x$  is largest for a strongly dispersive medium in which  $\epsilon$  has a rapid frequency dependence and the group velocity  $v'_{\text{gr}}$  results much slower than the vacuum speed of light  $v'_{\text{gr}} \ll c$ .

In this case, Galilean velocity composition laws can be safely applied and the result (18) simplifies to

$$\Delta x = \frac{Lv}{v'_{\text{gr}}}, \quad (22)$$

which yields a very intuitive interpretation for  $\Delta x$  as the displacement of the medium during the time interval  $\Delta t = L/v'_{\text{gr}}$  taken by the light to travel across it.

#### IV. THE TRANSVERSE FRESNEL-FIZEAU DRAG EFFECT IN A EIT MEDIUM

The first experimental observation of the transverse Fresnel-Fizeau drag effect was performed in the mid-1970's by Jones [31] using a rotating glass disk as moving dielectric medium. In such a non-dispersive medium the phase and group velocities were of the order of  $c$  ( $c/v'_{\text{gr}} \approx c/v'_{\text{ph}} \approx 1.5$ ) and the limited rotation velocity of the disk at the laser spot ( $v \simeq 2 \times 10^4 \text{cm/s}$ ) limited the lateral displacement to a distance of the order of 6 nm. However, a clever optical alignment technique allowed not only to observe the effect, but also to discriminate the validity of the result (15) from other possible expressions [32].

As remarked in the previous section, the use of a strongly dispersive medium allows for a significant enhancement of the drag effect. Very slow group velocities can now be obtained in both atomic samples [1, 2, 3, 4] and solid-state media [5, 6] by optically dressing a resonant transition with a coherent *coupling* laser beam as shown in the  $\Lambda$  level scheme of fig.2.

Under the assumption of a weak probe beam, linear response theory holds for the system dressed by the

<sup>4</sup> The assumed isotropy of the medium in its rest frame  $\Sigma'$  guarantees that group and phase velocities are always parallel in  $\Sigma'$ .

<sup>5</sup> Notice that in the rest frame  $\Sigma'$ , the beam waist appears as uniformly translating along the negative  $x$  axis. This unfamiliar feature however does not affect the argument.

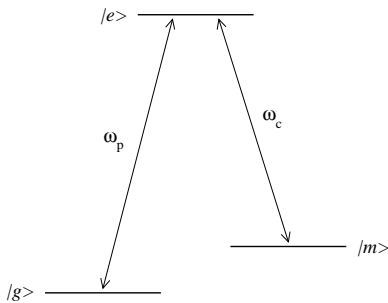


FIG. 2: Scheme of the energy levels involved in the optical transitions.

strong coupling beam: the resulting dielectric constant is to be interpreted as describing the linear response of the optically driven medium to the weak probe. Obviously, this dressed dielectric constant has a strongly nonlinear dependence on the coupling intensity so to account for all the nonlinear processes induced in the medium by the coupling field. In the simplest case of non-degenerate levels, the rest frame dielectric constant of our optically driven  $\Lambda$  configuration acquires the well-known form [11, 12, 13, 14],

$$\epsilon(\omega) = \epsilon_\infty + \frac{4\pi f}{\omega_e - \omega - i\gamma_e/2 - \frac{|\Omega_c|^2}{\omega_m + \omega_c - \omega - i\gamma_m/2}} \quad (23)$$

where  $\omega_{e(m)}$  and  $\gamma_{e(m)}$  are respectively the frequency and the linewidth of the excited  $e$  and metastable  $m$  states, where we have set  $\omega_g = 0$ . Here  $\omega_c$  is the frequency of the  $e \leftrightarrow m$  coherent coupling beam<sup>6</sup> and  $\Omega_c$  its Rabi frequency. The linewidth  $\gamma_m$  of the metastable state is much smaller than the linewidth  $\gamma_e$  of the excited state. The  $f$  parameter quantifies the oscillator strength of the optical transition: for an ultra cold atomic gas [1] at atomic densities  $n \approx 10^{12} \text{ cm}^{-3}$ ,  $f$  is of the order of a few  $10^{-3} \gamma_e$ . The background dielectric constant  $\epsilon_\infty$  takes into account the effect of all the other non-resonant transitions and for an atomic gas can be taken to be 1 to a very good approximation.

For a resonantly dressed medium, i.e.  $\delta_c = \omega_c - (\omega_e - \omega_m) = 0$ , the dielectric function (23) in the neighborhood of the resonance  $|\omega - \omega_e| \ll \gamma_e$  can be rewritten as:

$$\epsilon(\omega) = \epsilon_\infty + \frac{8\pi f i}{\gamma_e} \left[ 1 + \frac{2i\Omega_c^2/\gamma_e}{\omega_e - \omega - \frac{i}{2}(\gamma_m + \frac{4\Omega_c^2}{\gamma_e})} \right]. \quad (24)$$

In the imaginary part of this expression shown in fig.3a, it is easy to seize a narrow dip around  $\omega = \omega_e$  in the

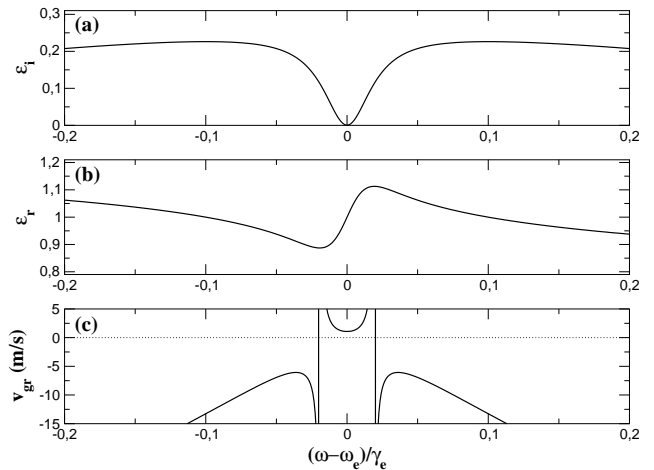


FIG. 3: Resonantly dressed EIT medium at rest: plot of the imaginary (a) and real (b) parts of the dielectric function  $\epsilon$  and of the group velocity  $v_{\text{gr}}$  (c). Medium parameters correspond to the case of an ultra cold  $^{23}\text{Na}$  gas:  $\gamma_e \simeq 2\pi \cdot 10 \text{ MHz}$ ,  $\lambda_e = 589 \text{ nm}$ ,  $f = 0.009 \gamma_e$ ,  $\epsilon_\infty = 1$ ,  $\gamma_m = 10^{-4} \gamma_e$ . The Rabi frequency of the resonant ( $\delta_c = 0$ ) coupling beam is  $\Omega_c = 0.1 \gamma_e$ . For this choice of parameters, the minimum (positive) group velocity is  $v_{\text{gr}} \approx 1 \text{ m/s}$ .

otherwise wide absorption profile of the  $g \rightarrow e$  transition. Provided  $\Omega_c^2/\gamma_e \gg \gamma_m$ , absorption at the center of the dip is strongly suppressed, yielding nearly perfect transparency for a resonant probe beam; this effect is the so-called *electromagnetically induced transparency* (EIT) effect [10]. The linewidth of the dip is  $\Gamma \simeq 4\Omega_c^2/\gamma_e$  and becomes strongly sub-natural ( $\Gamma \ll \gamma_e$ ) for  $\Omega_c \ll \gamma_e$ . The assumed inequality  $\gamma_m \ll \gamma_e$  guarantees that a good level of transparency can be obtained simultaneously with a sub-natural linewidth of the dip.

In the dip region, the real part (fig.3b) of the dielectric function (23) shows an extremely steep dispersion yielding the group velocity:

$$\frac{v_{\text{gr}}}{c} \simeq \frac{|\Omega_c|^2}{2\pi f \omega_e} \quad (25)$$

which can be orders of magnitude slower than the vacuum value  $c$  (fig.3c). This suggests that the importance of the transverse Fresnel-Fizeau drag effect (18) should be strongly enhanced in an EIT medium.

To verify this prediction, a complete calculation of the profile of the transmitted probe beam can be numerically performed by inserting the explicit expression of the dielectric function (23) into the dispersion law (6) and then performing the inverse Fourier transform (12). For a probe exactly on resonance with the  $g \rightarrow e$  transition ( $\omega_0 = \omega_e$ ), the numerical result plotted in fig.4a is in perfect agreement with the analytic prediction (18) when the value (25) for the group velocity is used. The near absence of absorption at the center of the dip guarantees that only a small fraction of the incident probe intensity is absorbed by the medium (fig.4b).

<sup>6</sup> Doppler shift of the coupling beam is avoided by choosing the direction of the coupling beam to be orthogonal to both the probe beam and the medium velocity. The waist of the coupling beam is taken as much larger than both the waist  $\sigma_0$  of the probe and the thickness  $L$  of the medium.

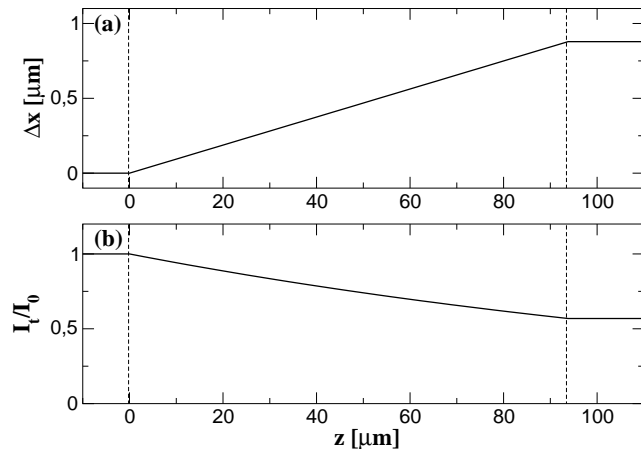


FIG. 4: Propagation of a light beam through a slowly moving ( $v = 0.01$  m/s), resonantly dressed EIT medium. The optical parameters of the medium are the same as in fig.3, the vertical dashed lines correspond to the surfaces of the medium, whose thickness is taken as  $L = 93 \mu\text{m}$ . The incident beam is resonant  $\omega_0 = \omega_e$  and its waist is  $\sigma_0 = 20 \mu\text{m}$ . *Downstream* transverse Fresnel-Fizeau drag (a) and corresponding weak absorption of the beam (b). The  $x$  axis is oriented in the downstream direction.

Group velocities as low as 1 m/s have been observed in ultra cold atomic gases. For the choice of parameters ( $v_{\text{gr}} = 1$  m/s and  $L \approx 100 \mu\text{m}$ ) made in fig.4, a medium velocity of the order of  $v = 0.01$  m/s gives a lateral shift of the order of  $\Delta x \approx 1 \mu\text{m}$ , orders of magnitude larger than the one originally observed by Jones [31, 32]. An even larger lateral shift  $\Delta x$  should be obtained by using a solid state material as dragging medium. Group velocities as slow as  $v_{\text{gr}} = 45$  m/s have in fact been recently observed in a Pr doped  $\text{Y}_2\text{SiO}_5$  [5] and Ruby [6] crystals. Furthermore, the mechanical rigidity and the possibility of working at higher temperatures should allow one to study the drag effect on a thicker sample moving at a higher speed  $v$ .

## V. ANOMALOUS TRANSVERSE FRESNEL-FIZEAU DRAG EFFECT

The discussion of the previous sections has focused on the most common case of media with *normal* dispersion. As Kramers-Kronig causality relations [39] ensure that

$$\frac{c}{v_{\text{gr}}} - \frac{v_{\text{ph}}}{c} > 0, \quad (26)$$

for all frequency regions at which the medium is transparent and non-amplifying, the corresponding transverse Fresnel-Fizeau drag (18) results directed in the *downstream* direction, as if the light were to be dragged by the moving medium.

On the other hand, several papers during the 70's [33, 34] have discussed the possibility of having an *upstream*

transverse Fresnel-Fizeau drag in the presence of *anomalous* dispersion, i.e. in the presence of negative group velocity. As negative group velocities in non-magnetic media are forbidden by Kramers-Kronig relations [39] in all frequency regions where the medium is transparent and non-amplifying, it has been possible to observe negative group velocities only in the presence of substantial absorption [40, 41, 42] or in amplifying media [43]. Notice that the negative group velocity effects which can be observed in left-handed media even in the absence of absorption arise from a completely different mechanism, that is from a simultaneously negative value of both the dielectric constant  $\epsilon$  and the magnetic susceptibility  $\mu$  [44]. This class of effects are excluded from the present discussion, which is limited to non-magnetic ( $\mu = 1$ ) materials.

In all experiments performed up to now, negative group velocities have been demonstrated by observing that the pulse advances in time with respect to the same wave packet propagating in vacuum. This kind of apparently superluminal behavior obviously refers to the peak of the wave packet only, and not to the propagation velocity of information; as discussed in the review [45], the velocity of the front of a step-function signal can never exceed  $c$ .

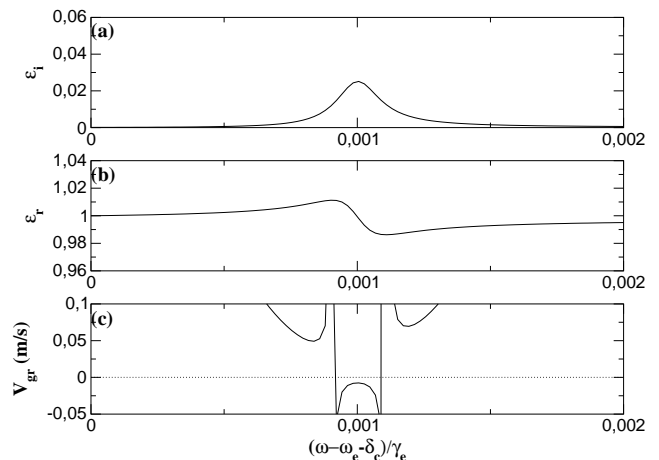


FIG. 5: Plot of the imaginary part  $\epsilon_i(\omega)$  of the dielectric function (a), of its real part  $\epsilon_r(\omega)$  (b), and of the group velocity  $v_{\text{gr}}(\omega)$  (c) for a non-resonantly ( $\delta_c = 10 \gamma_e$ ) dressed EIT medium at rest. The other parameters are the same as in fig.3.

As we have recently anticipated in [38], a significant upstream Fresnel-Fizeau drag effect should be observable in non-resonantly dressed EIT media, when the coupling beam is not exactly on resonance with the  $m \rightarrow e$  transition, but has a finite detuning  $|\delta_c| = |\omega_m + \omega_c - \omega_e| \geq \gamma_e$ . This kind of media have in fact been shown to be good candidates for the observation of ultra slow and negative group velocities [29]. In the case  $|\delta_c| \gg \gamma_e$ , the dielectric function (23) in the neighborhood of  $\omega = \omega_m + \omega_c$  (fig.5)

can be written in the Lorentzian form:

$$\epsilon(\omega) = \epsilon_\infty - \frac{4\pi f}{\delta_c} + \frac{4\pi f \Omega_c^2}{\delta_c^2} \frac{1}{\omega_2 - \omega - \frac{i}{2}(\gamma_m + \frac{\Omega_c^2 \gamma_e}{\delta_c^2})}. \quad (27)$$

Largest absorptions occur at the Raman resonance with the two-photon transition from the ground  $g$  state to the metastable  $m$  state via the excited  $e$  state, i.e. at the two-photon resonance frequency

$$\omega_2 = \omega_m + \omega_c + \frac{\Omega_c^2}{\delta_c}. \quad (28)$$

The shift  $\Omega_c^2/\delta_c$  from the bare resonant frequency is due to the optical Stark effect induced by the coupling beam. The linewidth of the resonance line is the sum of the bare linewidth of the metastable  $m$  level plus a contribution which takes into account its decay via the excited  $e$  state:

$$\gamma_2 = \gamma_m + \frac{\Omega_c^2}{\delta_c^2} \gamma_e. \quad (29)$$

For large coupling beam detunings  $|\delta_c| \gg \Omega_c$ , the linewidth  $\gamma_2$  results much smaller than the natural linewidth of the excited state, while the oscillator strength of the transition is itself weakened:

$$f_2 = \frac{\Omega_c^2}{\delta_c^2} f. \quad (30)$$

The peak absorption (proportional to  $f_2/\gamma_2$ ) does not vary for increasing values of  $|\delta_c|/\Omega_c$ , at least as far as  $\gamma_2 \gg \gamma_m$ . On the other hand, the anomalous dispersion at resonance  $\omega = \omega_2$  is under the same conditions enhanced due to the narrower linewidth  $\gamma_2$ . The corresponding group velocity is given by

$$\frac{v_{\text{gr}}}{c} = -\frac{\delta_c^2}{8\pi f \omega_e \Omega_c^2} \left( \gamma_m + \frac{\Omega_c^2}{\delta_c^2} \gamma_e \right)^2 \quad (31)$$

which, in the limit  $\gamma_2 \gg \gamma_m$ , is a factor  $\gamma_e^2/4\delta_c^2$  slower in magnitude than the one obtained in the resonant  $\delta_c = 0$  case considered in the previous section. This means that the use of a detuned coupling with  $|\delta_c| > \gamma_e$  should enable one to observe significant upstream drags over an optical thickness  $L$  of the order of the absorption length, so that the transmitted probe intensity still remains an appreciable fraction of the incident one.

In order to verify this expectation, we have again inserted the explicit expression of the dielectric function (23) into the propagation equation (6) and we have numerically performed the inverse Fourier transform so as to obtain the profile of the transmitted beam (fig.6a). As expected, light bendings are found to occur in the upstream direction and the magnitude of the effect is in good agreement with the approximated analytical expression (18) in which the imaginary part of  $\epsilon$  was neglected. We have also verified in fig.6b that the beam

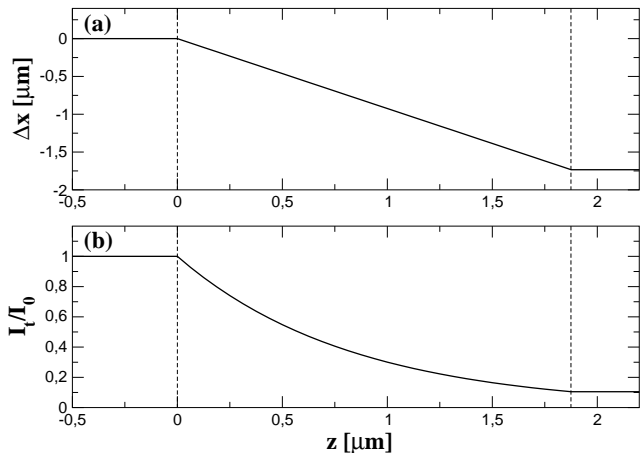


FIG. 6: Propagation of a light beam through a slowly moving ( $v = 0.01$  m/s), non-resonantly dressed ( $\delta_c = 10 \gamma_e$ ) EIT medium; probe frequency on resonance with the two-photon transition ( $\omega_0 = \omega_2$ ). The optical parameters of the medium are the same as in fig.5; the vertical dashed lines correspond to the surfaces of the medium, whose thickness is taken as  $L = 1.9 \mu\text{m}$ . The incident beam waist is  $\sigma_0 = 20 \mu\text{m}$ . Anomalous *upstream* transverse Fresnel-Fizeau drag (a) and corresponding absorption of the beam (b). The  $x$  axis is oriented in the downstream direction.

is not completely absorbed during propagation through the medium. Notice that for the same set of material parameters and the same experimental configuration as in the previous section, except for the coupling beam detuning  $\delta_c$ , the group velocity  $|v_{\text{gr}}|$  is now of the order of  $0.01$  m/s, i.e. a factor 100 slower than in the case of a resonant coupling. This explains the bigger deflection angle  $\theta$ .

Non-resonantly dressed EIT media are therefore good candidates for the experimental observation of significant upstream deflections and consequently large anomalous transverse Fresnel-Fizeau drags. Such an observation should finally resolve a controversy started in the seventies about the possibility of such an effect [33, 34]. Furthermore, the anomalous upstream Fresnel-Fizeau drag could also provide an interesting way of demonstrating negative group velocities, in alternative to the usual [40, 41, 42, 43] measurement of the negative temporal delay of the pulse after its propagation across the medium.

## VI. HIGHER ORDER DISPERSION EFFECTS

The effects discussed in the previous sections entirely rely on the strongly reduced value of the group velocity of light in EIT media. For slow enough medium velocities, higher order dispersion effects such as the dispersion of absorption or the group velocity dispersion are indeed very small and can be hardly observed in the results plotted in figs.4 and 6. On the other hand, these terms may

be no longer negligible for sufficiently large values of the medium velocity, regime in which the light propagation can exhibit qualitatively new features<sup>7</sup>. In the following of this section we shall discuss in detail two examples of such effects.

### A. Light propagation along a curved path

In the present subsection, we shall discuss the effect of non-rectilinear light propagation due to simultaneously large dispersions of both absorption [46] (proportional to  $d\epsilon_i/d\omega$ ) and group velocity (proportional to  $d^2\epsilon_r/d\omega^2$ ).

For large enough values of the absorption dispersion  $d\epsilon_i/d\omega$ , the absorption coefficient can have significant variations across the range of transverse  $k_x$  vectors present in the incident beam. In this case, the center of mass of the  $k_x$  wave-vector distribution

$$k_x^{\text{cm}}(z) = \frac{\int dk_x dk_y k_x |\tilde{E}(k_x, k_y; z)|^2}{\int dk_x dk_y |\tilde{E}(k_x, k_y; z)|^2} \quad (32)$$

moves from its initial value  $k_x^{\text{cm}}(z=0) = 0$  as the beam propagates through the medium. For a spatially wide Gaussian incident beam, we can limit the expansion of  $\epsilon_i$  to the linear terms in  $k_{x,y}$  and we find that the distribution of transverse wave vectors keeps a gaussian shape, but its center of mass  $k_x^{\text{cm}}(z)$  shifts to:

$$k_x^{\text{cm}}(z) = -\frac{z}{\sigma_0^2} \frac{\partial \text{Im}[k_z^{(in)}]}{\partial k_x} \quad (33)$$

For a negative value of  $\partial \text{Im}[k_z^{(in)}]/\partial k_x$ , the  $k_x > 0$  components result in fact less absorbed than the  $k_x < 0$  ones so that the Gaussian spectrum shifts towards the  $k_x^{\text{cm}} > 0$  region; vice versa for a positive value of  $\partial \text{Im}[k_z^{(in)}]/\partial k_x$ .

In the slow group velocity regime ( $v'_{\text{gr}} \ll c$ ), the dependence of the propagation wavevector (7) on the transverse wave vector  $k_{x,y}$  mainly comes from the Doppler effect combined with the strong frequency dispersion of the dielectric function, so that the transmission phase reads as:

$$\Phi(k_x, k_y; z) \simeq \frac{\omega_0 z}{c} \sqrt{\epsilon(\omega_0 - k_x v)}. \quad (34)$$

By applying the same stationary-phase arguments used in sec.III to the finite  $k_x^{\text{cm}}(z)$  case, we find that after

propagation for a distance  $z$  the spatial center of mass of the beam is located at

$$\Delta x(z) = z \frac{v}{v'_{\text{gr}}(\omega_0 - v k_x^{\text{cm}}(z))}. \quad (35)$$

In physical terms, as the spectral center of mass  $k_x^{\text{cm}}$  of the beam varies with  $z$  because of the filtering action of the absorption, the transverse Fresnel-Fizeau drag at a given position  $z$  has to be evaluated using the group velocity  $v'_{\text{gr}}$  at the Doppler shifted frequency  $\omega_0 - v k_x^{\text{cm}}(z)$ . In the presence of group velocity dispersion, the variation of  $k_x^{\text{cm}}(z)$  with  $z$  implies that the light beam is no longer rectilinear, but acquires a finite curvature. Notice in particular that the analytical expression for the angle  $\theta(z)$  between the trajectory (35) and the normal  $z$  direction

$$\begin{aligned} \tan \theta(z) &= \frac{\partial \Delta x(z)}{\partial z} = \\ &= \frac{v}{v'_{\text{gr}}(\omega_0 - v k_x^{\text{cm}})} + \frac{v^2 z}{[v'_{\text{gr}}(\omega_0 - v k_x^{\text{cm}})]^2} \frac{dv'_{\text{gr}}}{d\omega} \frac{dk_x^{\text{cm}}}{dz} \end{aligned} \quad (36)$$

now contains a term explicitly depending on the spectral center of mass shift  $dk_x^{\text{cm}}/dz$  which was not present in (15).

A related effect was discussed in the time domain in [47] where a small time-dependence of the group velocity for a light pulse propagating through a dispersive dielectric was predicted to show up as a consequence of the combined effect of the frequency dispersions of absorption and of group velocity.

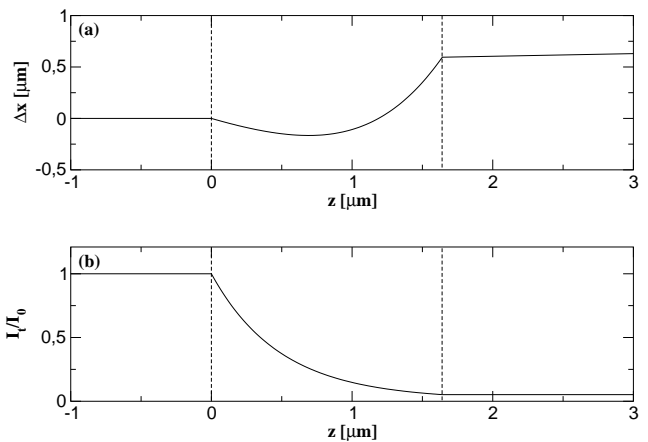


FIG. 7: Non-rectilinear light beam propagation through a moving ( $v = 4$  m/s) EIT medium for a resonant coupling ( $\delta_c = 0$ ) and a slightly detuned probe ( $\omega_0 - \omega_e = 0.04 \gamma_e$ ); the incident beam waist is  $\sigma_0 = 3 \mu\text{m}$ . (a) panel: curved beam path across the moving medium. (b) panel: intensity of the light beam at different depths in the medium. The optical parameters of the medium are the same as in fig.3; the vertical dashed lines correspond to the surfaces of the medium, whose thickness is taken as  $L = 1.65 \mu\text{m}$ .

<sup>7</sup> Even at the highest velocities here considered ( $v$  of the order of a few m/s), the use of the linearized form of the Lorentz transformations (3-5) is well justified: as the magnitude of the transverse Doppler effect of the probe and coupling beam  $|\Delta\omega_{\perp}| \simeq \omega_0 v^2/c^2 \lesssim 10^{-8} \gamma_e$  the contribution of the terms in  $v^2$  arising from the relativistic  $\gamma$  factor is negligible as compared to the one coming from the dispersion of  $\epsilon$ .

Figs.7-8, report the result of numerical calculations for the specific case of a moving EIT medium when the coupling beam is resonant ( $\delta_c = 0$ ) and the probe beam is



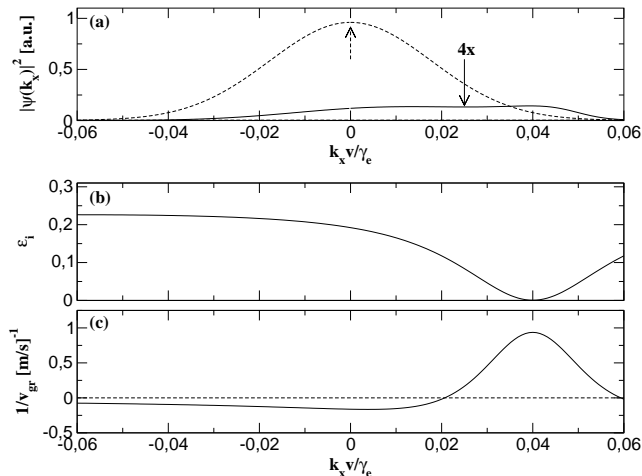


FIG. 8: Physical interpretation of the non-rectilinear light propagation of fig.7. (a) panel: spatial Fourier transform of the incident (dashed) and transmitted (solid) beam profile; for each spectrum, the arrow indicates the position of the spectral center of mass. For the sake of clarity, the transmitted spectrum has been multiplied by 4. (b) and (c) panels: absorption and inverse group velocity  $1/v_{gr}$  spectra as a function of the transverse wavevector  $k_x$ . The corresponding Doppler-shifted frequency in the rest frame  $\Sigma'$  is  $\omega' = \omega_0 - k_x v$ . Since  $\omega_0 - \omega_e = 0.04 \gamma_e$ , the resonance is found at  $k_x v = 0.04 \gamma_e$ .

slightly detuned towards the blue ( $\omega_0 - \omega_e = 0.04 \gamma_e$ ). As one can verify by comparing the spectrum in fig.8a with the group velocity spectrum in fig.8c, most of the incident beam spectrum lies in the negative group velocity region ( $k_x v < 0.02 \gamma_e$ ), so the beam is initially dragged in the upstream direction. As absorption is weaker for the  $k_x > 0$  components for which the Doppler-shifted frequency  $\omega' = \omega_0 - k_x v$  is closer to resonance ( $\partial \text{Im}[k_z^{(in)}] / \partial k_x < 0$ , see fig.8b), the negative  $k_x < 0$  components are more rapidly quenched than the positive  $k_x > 0$  components and the center of mass  $k_x^{(cm)}$  of the spectral distribution moves towards the positive  $k_x > 0$  values. As one can see in fig.8c,  $\frac{\partial}{\partial k_x} \frac{1}{v_{gr}} > 0$  in the region  $0 < k_x v < 0.04 \gamma_e$  of interest and therefore the curvature of the beam will be towards the downstream direction. After the first  $1 \mu\text{m}$  of propagation, most of the  $k_x$  spectrum is found in the positive  $v_{gr}'$  region ( $k_x v > 0.02 \gamma_e$ ), so that the transverse Fresnel-Fizeau drag is from now on in the downstream direction (fig.7a).

As a consequence of the shift of the spectral center of mass  $k_x^{cm}$ , the beams exits from the rear face of the medium at a small but finite angle with respect to the normal towards the downstream direction. Although this effect is hardly visible on the scale of fig.8a, this small bending of the beam direction may have a significative effect on the subsequent rectilinear propagation of the beam in the free space.

Unfortunately, this effect of non-rectilinear propagation is associated to a rather severe absorption of the beam; for the specific case in figure, the transmitted in-

tensity is of the order of 5% of the incident one (fig.7b).

It is also worth noticing that the curvature effect described in the present section follows from a reshaping of the beam in momentum space and hence is physically different from the ones discussed in [22, 23], which instead originate from a non-uniform velocity field of the slow-light medium.

## B. Temporal and spatial coherence restoration

If both probe and coupling beams are exactly on resonance ( $\omega_0 - \omega_e = \delta_c = 0$ ), both absorption  $d\epsilon_i/d\omega'$  and group velocity  $d^2\epsilon_r/d\omega'^2$  dispersion vanish, so that the effects described in sec.VIA do not take place. In the present subsection, we shall show how one can rather take advantage of the large value of  $d^2\epsilon_i/d\omega'^2$  to improve the coherence level of a noisy incident probe beam. In sec.VIB 1, the case of *temporal* coherence restoration in a stationary EIT medium will be addressed, while in sec.VIB 2 we shall show how the same concepts can be applied in the case of a moving EIT medium to improve the level of *spatial* coherence.

### 1. Temporal coherence restoration

Consider an incident probe beam of carrier frequency  $\omega_0$  whose complex amplitude  $E_0(t)$  is assumed as fluctuating in time over a characteristic time scale  $\tau_c$ :

$$E(t) = E_0(t) e^{-i\omega_0 t}. \quad (37)$$

Following a standard model [48], the decay in time of the first-order coherence function  $g^{(1)}(\tau)$  is taken to be Gaussian:

$$g^{(1)}(\tau) = \frac{\langle E_0^*(\tau) E_0(0) \rangle}{\langle E_0^*(0) E_0(0) \rangle} = \exp(-\tau^2/2\tau_c^2). \quad (38)$$

The frequency spectrum  $|\tilde{E}(\omega)|^2$  of the beam, being proportional to the Fourier transform of the coherence function  $g^{(1)}(\tau)$ , is also Gaussian with linewidth  $\sigma_c = 1/\tau_c$ .

In a one-dimensional geometry, the propagation of a pulse through a stationary dielectric medium is described by the usual Fresnel equation:

$$k_z^2(\omega) = \epsilon(\omega) \frac{\omega^2}{c^2}. \quad (39)$$

In the neighborhood of the resonance at  $\omega_e$ , the dielectric function of a slow light EIT medium can be approximately written as:

$$\epsilon(\omega) \simeq 1 + \frac{2c}{\omega_e v_{gr}} (\omega - \omega_e) + i \frac{\alpha}{2} (\omega - \omega_e)^2 \quad (40)$$

where  $v_{gr}$  is the group velocity at resonance and the real quantity  $\alpha$  is given by:

$$\alpha = \left. \frac{d^2 \epsilon_i(\omega)}{d\omega^2} \right|_{\omega=\omega_e} = \frac{4\pi f \gamma_e}{\Omega_c^4}. \quad (41)$$

At the lowest order in  $\omega - \omega_e$ , the real and imaginary parts of the wavevector  $k_z(\omega)$  can then be written as:

$$k_z(\omega)|_r \simeq \frac{\omega_e}{c} \left[ 1 + \frac{c}{\omega_e v_{gr}} (\omega - \omega_e) \right]. \quad (42)$$

$$k_z(\omega)|_i \simeq \frac{\alpha \omega_e}{4c} (\omega - \omega_e)^2 \quad (43)$$

In particular, notice how the imaginary part of  $k_z$  is proportional to the square of  $\omega - \omega_e$ . Since after propagation over a distance  $L$  the amplitude of each frequency component is multiplied by a factor  $\exp[ik_z(\omega)L]$ , the frequency spectrum after propagation keeps its Gaussian shape, but the frequency linewidth is reduced to:

$$\sigma_c(L) = \frac{\sigma_c}{\sqrt{1 + \frac{\alpha \sigma_c^2 \omega_e}{c} L}} \quad (44)$$

and the coherence time correspondingly increased to:

$$\tau_c(z) = \tau_c \sqrt{1 + \frac{\alpha \omega_e}{c \tau_c^2} L}. \quad (45)$$

Since the EIT medium does not provide amplification, a drawback of this filtering technique is that part of the incident intensity is lost during the line-narrowing process; the beam intensity after propagation through a distance  $L$  is in fact equal to:

$$I(L) = \frac{\sigma_c(L)}{\sigma_c(0)} I(0). \quad (46)$$

## 2. Spatial coherence restoration

For a moving EIT medium and a strictly monochromatic light beam at  $\omega_0$ , a similar effect occurs in the  $k_x$  space. As discussed in full detail in sec.II, the propagation of light is described in this case by equation (7). For resonant probe and coupling beams, the imaginary part of  $\text{Im}[k_z^{(in)}]$  corresponding to absorption is proportional to  $v^2 k_x^2$ :

$$\text{Im}[k_z^{(in)}] \simeq \frac{\alpha \omega_0}{4c} v^2 k_x^2. \quad (47)$$

As the amplitude of the transverse spatial fluctuations is proportional to the amplitude of non-vanishing  $k_x$  components, the spatial profile of the beam flattens as the beam propagates through the moving EIT medium. The faster the speed  $v$  of the medium, the more efficient the spatial coherence restoration process.

Results of a numerical calculation for a spatially noisy incident beam propagating through a moving EIT medium are presented in fig.9. Notice how the fluctuation amplitude is strongly suppressed during propagation. At the end of the process, the losses in the total intensity amount to 60%.

The overall shift of the beam which can be seen in the figure is due to the transverse Fresnel-Fizeau drag effect discussed in detail in sec.IV. Since both the probe and the coupling are resonant, the shift is directed in the downstream direction.

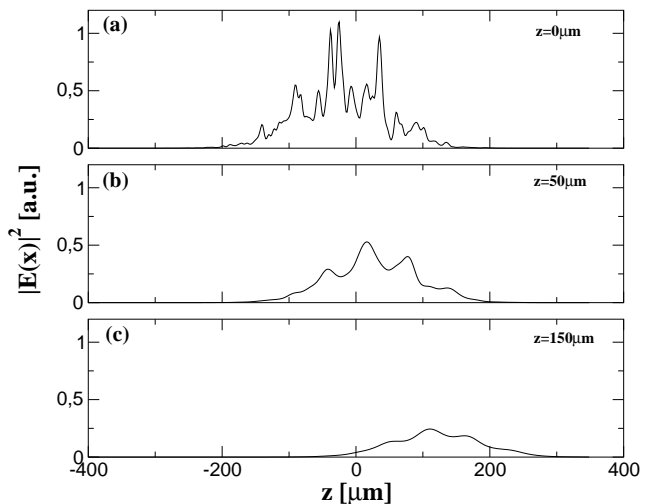


FIG. 9: Transverse spatial coherence restoration during propagation across a moving ( $v = 1$  m/s) EIT medium in a fully resonant regime ( $\delta_c = \omega_0 - \omega_e = 0$ ,  $\omega_0 = \omega_e$ ). (a) panel: noisy incident beam profile. (b,c) panels: beam profile after propagation through the medium. Same medium parameters as in fig.3-7.

## VII. CONCLUSIONS

In the present paper we have given a comprehensive analysis of the transverse Fresnel-Fizeau drag effect for light propagating across a uniform slab of moving EIT medium. All calculations have been performed using realistic parameters taken from EIT experiments with ultra-cold atomic clouds. Since our results are essentially a consequence of electromagnetically induced transparency, they are extremely general and thus hold through also for the recently prepared solid state EIT media. Depending on the detuning of the probe and coupling beams with respect to the medium resonance, different regimes have been identified.

In the presence of a slow and positive group velocity, the magnitude of the downstream Fresnel-Fizeau drag effect is predicted to be significantly enhanced with respect to previous experiments. In the regime of negative group velocity, an anomalous upstream Fresnel-Fizeau drag has been predicted to occur. Not only would this help in solving a long-standing controversy on the observability of such an effect, but it could also provide an interesting alternative way for experimentally detecting a negative group velocity.

For larger values of the velocity of the moving medium, higher order dispersion terms such as the dispersion of absorption and the dispersion of group velocity have been shown to play an important role in the phenomenology of light propagation. Depending on the specific choice of probe and coupling detuning, light propagation along curved paths can be observed, as well as the restoration of spatial coherence of a noisy beam.

The extension of the present analysis to more compli-

cated geometries including non-uniformly moving slow light media as well as probe pulses of finite duration will be the subject of future studies.

### Acknowledgments

One of us (M.A.) should like to thank U. Leonhardt for enlightening discussions on the issue of slow

light in moving media. Financial support from the EU (Contracts HPMF-CT-2000-00901 and HPRICT1999-00111), from the INFM (project PRA "photonmatter") and from the MIUR (grant PRIN 2002-028858) is greatly acknowledged. Laboratoire Kastler Brossel is a unité de Recherche de l'École normale supérieure et de l'Université Pierre et Marie Curie, associée au CNRS.

- 
- [1] L. V. Hau, S. E. Harris, Z. Dutton, and C. H. Behroozi, *Nature* **397**, 594 (1999);
- [2] S. Inouye *et al.*, *Phys. Rev. Lett.* **85**, 4225 (2000).
- [3] M. M. Kash *et al.*, *Phys. Rev. Lett.* **82**, 5229 (1999);
- [4] D. Budker, D. F. Kimball, S. M. Rochester, and V. V. Yashchuk, *Phys. Rev. Lett.* **83**, 1767 (1999).
- [5] A. V. Turukhin *et al.*, *Phys. Rev. Lett.* **88**, 023602 (2002).
- [6] M. S. Bigelow, N. N. Lepeshkin, and R. W. Boyd, *Phys. Rev. Lett.* **90**, 113903 (2003).
- [7] O. Kocharovskaya, Y. Rostovtsev, and M. O. Scully, *Phys. Rev. Lett.* **86**, 628 (2001).
- [8] D. F. Phillips *et al.*, *Phys. Rev. Lett.* **86**, 783 (2001);
- [9] C. Liu, Z. Dutton, C. H. Behroozi, and L. V. Hau, *Nature*, **409**, 490, (2001).
- [10] G. Alzetta, A. Gozzini, L. Moi, and G. Orriols, *Nuovo Cimento* **36B**, 5 (1976); E. Arimondo, G. Orriols, *Lett. Nuovo Cimento* **17**, 333 (1976).
- [11] E. Arimondo in *Progress in Optics XXXV*, ed. by E. Wolf, Elsevier Science, (1996) pag.257.
- [12] T.W. Hänsch, P.E. Toschek, *Z. Phys.* **236**, 213 (1970).
- [13] S. Harris, *Phys. Today* **50**, No. 7, 36 (1997).
- [14] A. B. Matsko *et al.*, *Adv. At. Mol. Opt. Phys.* **46**, 191 (2001).
- [15] J. Marangos, *J. Mod. Opt.* **45**, 471 (1998).
- [16] S. E. Harris, J. E. Field, and A. Kasapi, *Phys. Rev. A* **46**, R29 (1992);
- [17] S. E. Harris and L. V. Hau, *Phys. Rev. Lett.* **82**, 4611, (1999);
- [18] M. D. Lukin and A. Imamoglu, *Phys. Rev. Lett.* **84**, 1419 (2000).
- [19] M. D. Lukin, S. F. Yelin, and M. Fleischhauer, *Phys. Rev. Lett.* **84**, 4232 (2000).
- [20] M. Fleischhauer and M. D. Lukin, *Phys. Rev. Lett.* **84**, 5094 (2000).
- [21] A. B. Matsko, Y. V. Rostovtsev, H. Z. Cummins, and M. O. Scully, *Phys. Rev. Lett.* **84**, 5752 (2000).
- [22] U. Leonhardt and P. Piwnicki, *Phys. Rev. Lett.* **84**, 822 (2000);
- [23] U. Leonhardt, *Phys. Rev. A* **62**, 012111 (2000);
- [24] U. Leonhardt and P. Piwnicki, *J. Mod. Opt.* **48**, 977 (2001);
- [25] U. Leonhardt, *Phys. Rev. A* **65**, 043818 (2002);
- [26] U. Leonhardt, *Nature* **415**, 406 (2000);
- [27] J. Fiurasek, U. Leonhardt and R. Parentani, *Phys. Rev. A* **65**, 011802 (2002);
- [28] U. Leonhardt, *Phys. Rev. A* **62**, 012111 (2000). *Physics World*, **15**, No 2, 7, (2002)
- [29] M. Artoni, G. C. La Rocca, F. S. Cataliotti, and F. Bassani, *Phys. Rev. A* **63**, 023805 (2001).
- [30] M. Artoni, I. Carusotto, G. C. La Rocca, and F. Bassani, *Phys. Rev. Lett.* **86**, 2549 (2001).
- [31] R. V. Jones, *Proc. Roy. Soc. London A* **328**, 337 (1972).
- [32] R. V. Jones, *Proc. Roy. Soc. London A* **345**, 351 (1975).
- [33] H. C. Ko and C. W. Chuang, *Astroph. Journ.* **222**, 1012 (1978); H. C. Ko, *Astroph. Journ.* **231**, 589 (1979).
- [34] I. Lerche, *Astroph. Journ.* **187**, 589 (1974).
- [35] J. D. Jackson, *Classical Electrodynamics* (J. Wiley, New York, 1975).
- [36] M. A. Player, *Proc. Roy. Soc. London A* **345**, 343 (1972).
- [37] G. L. Rogers, *Proc. Roy. Soc. London A* **345**, 345 (1972).
- [38] M. Artoni, I. Carusotto, G. C. La Rocca, and F. Bassani, *J. Opt. B* **4**, S345 (2002).
- [39] L. D. Landau and E. M. Lifshitz, *Electrodynamics of continuous media*, Pergamon Press, London, 1960.
- [40] S. Chu and S. Wong, *Phys. Rev. Lett.* **48**, 738 (1982);
- [41] A. M. Steinberg, P. G. Kwiat, and R. Y. Chiao, *Phys. Rev. Lett.* **71**, 701 (1993);
- [42] Ph. Balcou and L. Dutriaux, *Phys. Rev. Lett.* **78**, 851 (1997).
- [43] L. J. Wang, A. Kuzmich, and A. Dogariu, *Nature* **406**, 277 (2000).
- [44] V.G.Veselago, *Sov. Phys. Usp.* **10**, 509 (1968); D.R.Smith, *et al.*, *Phys. Rev. Lett.* **84**, 4184 (2000)
- [45] P. W. Milonni, *J. Phys. B: At. Mol. Opt. Phys.* **35**, R31 (2002).
- [46] M. Artoni and R. Loudon, *Phys. Rev. A* **55**, 1347 (1997).
- [47] L. Muschietti and C. T. Dum, *Phys. Fluids B* **5**, 1383 (1993).
- [48] R. Loudon, *The quantum theory of light*, Clarendon Press, Oxford, 1973.